Ocean acidification does not affect magnesium composition or dolomite formation in living crustose coralline algae, *Porolithon onkodes* in an experimental system

Nash, M.C[1] Uthicke[2], S, Negri[2], A. P., Cantin[2], N. E.*

[1]*Research School of Physics, Australian National University*

[2]*Australian Institute of Marine Science, Townsville, Queensland*

*corresponding author: merinda.nash@anu.edu.au

Abstract

There are concerns that Mg-calcite crustose coralline algae (CCA), which are key reef builders on coral reefs, will be most susceptible to increased rates of dissolution under higher pCO_2 and ocean acidification. Due to the higher solubility of Mg-calcite, it has been hypothesized that magnesium concentrations in CCA Mg-calcite will decrease as the ocean acidifies, and that this decrease will make their skeletons more chemically stable. In addition to Mg-calcite, CCA *Porolithon onkodes* the predominant encrusting species on tropical reefs, can have dolomite ($Ca_{0.5}Mg_{0.5}CO_3$) infilling cell spaces which increases their stability. However, nothing is known about how bio-mineralised dolomite formation responds to higher pCO_2. Using *P. onkodes* grown for 3 and 6 months in tank experiments, we aimed to determine 1) if mol% $MgCO_3$ in new crust and new settlement was affected by increasing CO_2 levels (365, 444, 676 and 904µatm), 2) whether bio-mineralised dolomite formed within these time frames, and 3) if so, whether this was effected by CO_2. Our results show there was no significant affect of CO_2 on mol% $MgCO_3$ in any sample set, indicating an absence of a plastic response under a wide range of experimental conditions. Dolomite within the CCA cells formed within 3 months and dolomite abundance did not vary significantly with CO_2 treatment. While evidence mounts that climate change will impact many sensitive coral and CCA species, the results from this study indicate that reef-building *P. onkodes* will continue to form stabilising dolomite infill under near-future acidification conditions, thereby retaining its higher resistance to dissolution.

1 Introduction

Determining the influence of ocean acidification from increasing CO_2 concentrations on mineral formation of crustose coralline algae (CCA) is not only important to understand potential changes in CCA and their reef building capacity in the future, but also to understand the past. As atmospheric carbon dioxide (CO_2) concentrations increase, fundamental changes to the ocean's chemistry follow. Seawater pH and the carbonate saturation state (Ω) decrease, thus increasing the solubility of $CaCO_3$ skeletons. Current projections are that by the end of this century, if anthropogenic CO_2 emissions continue unabated, tropical surface seawater pH will drop by 0.3-0.4 units to ~ pH 7.8 (Orr 2011). Marine organisms forming carbonate skeletons are susceptible to increased rates of dissolution as pH declines (reviewed in Howard et al., 2012). There are concerns that CCA will be one of the first reef-building organisms to suffer as CO_2 rises (e.g. Diaz-Pulido et al., 2012), due to the higher solubility of their skeleton. The possibility has also been raised that CCA may decrease their uptake of Mg to form more stable lower Mg-calcite in response to higher CO_2 concentrations (e.g. Andersson et al., 2008; Ries 2011).

Experimental data on the impacts of pH on Mg uptake by tropical CCA are limited. The branching coralline *Neogoniolithon* demonstrated a decreased magnesium concentration in severely low pH conditions (Ries 2011). However, CCA *Porolithon onkodes* transplanted into low pH treatments for 8 weeks did not exhibit any Mg composition change with pH in new surface tissue (Diaz-Pulido et al., 2014). Temperate coralline *Corallina elongate* had a variable response with new growth on existing branches not exhibiting a response to elevated CO_2 whereas new structures grown during the experiment did have decreased Mg content in higher CO_2 treatments (Egilsdottir et al., 2012). Temperate rhodoliths *Lithothamnion glaciale* did not change Mg content in different CO_2 treatments while living. However, a significant decrease in the Mg content in low pH compared to dead thalli in the same treatment raised the possibility that there was a biological response (Kamenos et al., 2013). Recently it was discovered that tropical CCA *P. onkodes* commonly possess additional Mg minerals dolomite ($Mg_{0.5}Ca_{0.5}CO_3$) and magnesite ($MgCO_3$) infilling cells in the crust (Nash et al., 2011). This additional mineralisation significantly reduces rates of skeletal dissolution compared to *P. onkodes*

without dolomite cell infill (Nash et al., 2013a). A combination of high CO_2 and increased temperature over 8 weeks led to a ~300% increase in the relative quantity of dolomite in *P. onkodes* crust transplanted into the treatment conditions (Diaz-Pulido et al., 2014). This was due to endolithic cyanobacteria, *Mastigocoleus* sp, removing calcium from the Mg-calcite skeleton but not from dolomite, leading to destruction of Mg-calcite and a relative increase in dolomite. It could not be determined if there was also an increase in the formation of primary dolomite.

When CCA grow to form the thick crust crucial to cementing together the structural reef framework, the new growth extends upwards leaving the old growth as a white crust without pink photosynthetic pigment. The pink surface of the CCA is the epithallus and the pink colouration is due to the presence of pigmented photosynthetic tissue within the Mg-calcite skeleton. In other species of corallines, this pink surface has been shown to slough off (Pueschel et al., 2005) and be grazed by chitons and limpets (Adey et al., 2013). The white crust underneath (perithallus) has been shown in other species of CCA to form as cell by cell growth downward from the meristem cells (growth layer between epithallus and perithallus) (Adey et al., 2013). Thus the white crust is a product of meristem growth, and not a build up of epithelial growth after it looses its pigmentation It is in this important reef-structure forming white crust that dolomite infill is abundant (Nash et al., 2011; Diaz-Pulido et al., 2014). As yet, there have been no experiments to determine the impact of CO_2 levels on mol% $MgCO_3$ and dolomite formation in the white crust grown in differing CO_2 treatments.

There is a noted correlation of sedimentary dolomite abundance and greenhouse conditions (high temperature, high CO_2) over the geological past (e.g. MacKenzie et al., 2008; Wilkinson and Given 1986). To understand the past, it is necessary to separate the roles that CO_2 and temperature may have had on constraining dolomite concentration. Bio-mineralised dolomite has been found in modern environments (Vasconcelos and Mackenzie 1997; Nash et al., 2011), but it is not known how changes in CO_2 concentrations may affect formation of bio-mineralised dolomite. This study describes

92 the first experiments that constrain the role of CO_2 on CCA bio-mineralised dolomite
93 formed in differing CO_2 environments.
94
95 The aims of this investigation were threefold; 1) to identify any changes in mol% $MgCO_3$
96 in new settlement and new white crust of *P. onkodes* grown in Pre-industrial, Control
97 (present day), Medium (near future) and High (end of century) CO_2 (IPCC, 2007)
98 conditions over 3 and 6 months; 2) to determine whether CCA bio-mineralised dolomite
99 is formed within these timeframes; 3) to determine if the CO_2 concentration affects CCA
100 bio-mineralised dolomite formation.
101

102 2 Methods

103 2.1 Experiment

104 Fragments of live *P.* onkodes were collected from the upper reef crests (2 – 3 m depth) of
105 Davies Reef (18°49.29'S, 147°37.99'E), Great Barrier Reef in August 2012. To
106 eliminate open carbonate surfaces, CCA chips (~1 cm diameter) were sealed around the
107 sides and base in non-toxic under water glue (Mr. Sticky's, Fair Oaks, CA) and attached
108 to PVC slides (only the top live surfaces were exposed to seawater). Blank slides were
109 also added to the system to identify and track new CCA settlement. Slides were mounted
110 in custom perspex holders which were held in place on aquarium walls using magnets.
111 The experimental system used was described in (Uthicke et al.,, 2013). Briefly, fresh
112 filtered seawater (0.4 mm) was added to three replicate tanks (for each treatment)
113 replacing the water twice daily. Flow rates in each experimental tank were 12 L min^{-1}. In
114 addition to a present day (pH_T 8.0 target, measured mean 7.96 +/- 0.04 SE CO_2: 444 +/-
115 37 µatm), mid-century 2050 (future pH_T 7.9 target, measured mean 7.90 +/- 0.04 SE CO_2:
116 676 +/- 37µatm) and end of century 2100 (future pH_T 7.75 target, measured mean 7.77
117 +/- 0.06 SE CO_2 904 +/- 32µatm) target acidification treatments, this experiment also
118 included a pre-industrial treatment (past pH_T 8.14 target, measured mean 8.09 +/- 0.04 SE
119 CO_2: 365 +/- 37µatm). Acidified treatments were achieved by bubbling CO_2 into sump
120 tanks with solenoid valves (SMC pneumatics) and controlled with pH setpoints, while the
121 pre-industrial treatment was achieved by passing a stream of atmospheric air through 2
122 soda lime canisters and mixing the low CO_2 scrubbed air with the incoming seawater in a

123 counter current exchange tower prior to flowing into each experimental tank.
124 Temperatures were controlled (Avg. 26.1 ± 0.15°C) with a heater chiller unit (EvoHeat
125 DHP40). pH and temperature were monitored continuously (30 sec sampling rate) with
126 ISFET type pH probes (Endress Hauser CPS-471D). Seawater CO_2 concentrations were
127 measured using a LiCor (LI-840A) CO_2/H_2O analyser. This experiment was conducted
128 within the outdoor aquarium facility at the Australian Institute of Marine Science under
129 natural daily light cycles during the Austral summer (October-April). Outdoor light
130 intensities were reduced with 70% UV blocking green shade cloth to an average intensity
131 of 210 ± 12 µmol photons m^{-2} s^{-1}, with a daily maximum of 330 µmol photons m^{-2} s^{-1}.
132 These light intensities correspond to the daily average light intensity on shallow reefs.
133
134 **2.2 Sample selection**
135 Subsets of CCA's in resin were removed from the tanks after 3 and 6 months. The
136 settlement slides were removed after 6 months. Samples were randomly selected from
137 these for XRD analyses. New crust from the resin-embedded CCA's was sampled by
138 breaking off the crust that overgrew the resin. This ensured that only crust formed during
139 the experiment was included in the new crust analyses. The new crust typically had a thin
140 layer (~0.5 to 2 mm) of white crust overlain by a layer of pink photosynthetic epithallus
141 (Figure 1). CCA that had settled on the plastic slides after 6 months had only pink crust
142 and there was no white crust underneath. Typically for the new settlement CCA, 2-4
143 settlement patches were required to obtain sufficient material for analysis by XRD, thus
144 each individual result for new settlement is an average of several CCA patches. These
145 CCA had not reached reproductive stage and could not be identified. For the 6 month
146 experiment, CCA's in resin from the control tanks were unavailable for mineral analysis.
147 **2.3 Analyses**
148 CCA were cut using a bench-top saw with a 2 mm thick diamond impregnated blade. A
149 slice through the middle of each 3-month sample was kept for SEM. Scanning Electron
150 Microscopy-Energy Dispersive Spectroscopy (SEM-EDS) was undertaken at the
151 Australian National University using a Ziess UltraPlus field emission scanning electron
152 microscope (FESEM) equipped with an HKL electron backscatter diffraction (EBSD)
153 operated at 15kV, 11 mm working distance. CCA were mounted using carbon tape and

carbon coated. Subsampling for XRD was taken from the matching side of the remainder crust. Samples (>20 mg) were milled by hand in an agate mortar. Fluorite was added as an internal standard. Acetone was not used as this has been found to react with the pink pigmented surface samples. Samples were mounted onto quartz low background holders. Scan range was 25-33° 2-theta, step size 0.02° 2-theta and a scan speed of 1°/min. Xray diffraction and mineral determination was carried out following Nash et al., (2013b). Simply, this method uses the asymmetry off the higher 2-theta side of the Mg-calcite XRD peak to detect dolomite. The more asymmetry the greater proportion of dolomite in the crust. A shoulder off the higher 2-theta side of the peak indicates magnesite ($MgCO_3$) is also present. This asymmetry and shoulder is captured with the asymmetry mol% measurement. The asymmetry mol% is used to compare for differences in relative dolomite and magnesite quantities (Nash et al., 2013b). It is not a measurement of absolute quantity. However, when compared to mineral quantities determined using standard curve fitting techniques, the differences in asymmetry well reflect the differences in dolomite and magnesite quantities (as used in Diaz-Pulido et al., 2014). See Figure 1 (Supplement) for example scans.

2.4 Dolomite terminology

Stoichiometric dolomite is 50 mol% $MgCO_3$. Typically dolomite formed under high temperature is stoichiometric and well ordered (Kaczmarek and Sibley 2011). Ordering occurs where there are alternating layers of $MgCO_3$ and $CaCO_3$ in the calcite lattice, whereas completely disordered dolomite has Mg randomly substituting for Ca in the lattice. Sedimentary dolomite formed at sea surface temperature and pressure and not subject to post-deposition burial and metamorphism, typically is non-stoichiometric with a range of 37.5 to 52 mol% $MgCO_3$ (Jones et al., 2001) and not well ordered (Kaczmarek and Sibley 2011). Synthetically formed disordered dolomite has been shown to be unstable in aqueous solutions and therefor it is thought that disordered dolomite cannot form or persist in the open marine environment in which sedimentary dolomite forms (Gaines 1977). A variety of descriptions exist for dolomite that deviates from stoichiometric and perfectly ordered; non-ideal, poorly ordered or disordered, protodolomite, pseudo-dolomite and calcium enriched dolomite (Gaines 1977).

Here we use the term dolomite to represent magnesium calcite in the range 38-62 mol% $MgCO_3$, as measured for *P. onkodes* dolomite (Nash et al., 2011) without inferring cation ordering status, that is, whether it is ordered, disordered or partially ordered. The *P. onkodes* dolomite has previously been demonstrated via etching experiments and natural dissolution processes to have a delayed dissolution reaction compared to Mg-calcite and has different crystal forms to Mg-calcite (Nash et al., 2013a). Furthermore, it has been documented that Mg-calcite in *P. onkodes* ranges up to ~26 mol% $MgCO_3$ (Nash et al., 2011) and there is a well-defined division from dolomite which commences at ~38 mol% $MgCO_3$. Experimental work has demonstrated that cyanobacteria (*Mastigocoleus* sp) which bio-erode limestone by removing calcium, do not take calcium from dolomite rock (Ramirez-Reinat and Garcia-Pichel 2012). Experiments on live dolomite-forming *P. onkodes* also show that the same cyanobacteria remove calcium from Mg-calcite but do not remove calcium from the *P. onkodes* dolomite. *P. onkodes* Mg-C and *P. onkodes* dolomite have distinctly different physical properties and *P. onkodes* dolomite reacts under chemical (Nash et al., 2013a) and bio-erosion conditions (Diaz-Pulido et al., 2014) comparably to dolomite the rock. We have been unable to confirm the presence of ordering peaks by XRD for the dolomite within the living *P. onkodes* (Nash et al., 2013b). However, the persistence of the CCA dolomite in aqueous environments and its greater resistance to dissolution than Mg-calcite (Nash et al., 2013a) suggests there is some degree of ordering and *P. onkodes* dolomite is not the same mineral as Mg-calcite which theoretically becomes less stable with greater Mg-substitution (Andersson et al., 2008). Therefore, we consider that referring to the CCA mineral as dolomite, with the caveat that this is without inferring cation-ordering status is the most appropriate identification for the mineral at this time. Our decision to use this terminology for Mg-C > 38 mol % $MgCO_3$ is supported by recently published clarification on terminology for Ca-Mg carbonates (Zhang et al., 2015).

2.5 Crust terminology

The term 'pre-experimental growth' refers to crust grown in situ at Davies reef prior to collection for the experiment. The new crust (experimental) is the growth above the height of the resin. The 'new crust' terminology is used because this includes both the white crust of the perithallus and the pink surface epithallus. There may also be re-growths within the white crust that includes hypothelial cells and alteration to aragonite (see for example Fig. 8). The new settlement on slides in the 6 month treatment was predominantly pink indicating epithelial growth. However, when CCA settle, the first cells laid down are hypothelial cells growing lengthways parallel to the surface and then vertical growth of the epithallus, followed by the perithallus (Steneck 1986). A scraping sample would include not only epithallus but also minor hypothallus and possibly the start of a perithallus. For this reason we use the term new settlement rather than epithallus

2.5 Statistical analysis

We tested for differences between CO_2 treatments and sample type using two factor analysis of variance (ANOVA). Different CO_2 treatments (Factor Treatment) and experimental growth versus pre-experimental growth (Factor Type) were both used as fixed factors. Residual plots and boxplots confirmed that there were no deviations from ANOVA assumptions. Because slightly unequal sample sizes were used in each treatment, we applied marginal sums of squares for the F-tests.

3 Results

3.1 Mineral composition in different CO_2 treatments

We investigated the mineral composition of CCA exposed to different OA conditions for 3 and 6 months in a long-term aquarium experiment. There were no significant differences in mineral composition between any of the CO_2 treatments (Table 1). For the new *P. onkodes* crust formed during the 3 month duration (Figure 2a), the mol% $MgCO_3$ range is 16.4 – 16.7 mol% $MgCO_3$ (n = 5 per treatment, averages: Pre 16.6, Control 16.5, Medium 16.4, High 16.7 mol% $MgCO_3$) (full results supplement Table 1). This range is only 0.1 mol% more than measurement precision (Nash et al., 2011). For the new *P. onkodes* crust formed over 6 months (Fig. 2b), the mol% $MgCO_3$ range was the same as the 3 month crust 16.4 – 16.7 mol% $MgCO_3$, (Pre 16.7 n=5, Medium 16.4 n=3, High 16.5

mol% $MgCO_3$ n=6) (Supplement Table 2). Many of the Mg-calcite XRD peaks for both the 3 and 6 month crust demonstrated asymmetry indicating the presence of dolomite (as per Nash et al., 2011, 2012, 2013a,b, Diaz-Pulido et al., 2014). There was no significant difference in the dolomite asymmetry related to CO_2 treatments (asymmetry test, Table 1). For unidentified CCA that had settled on the slides over 6 months (Fig. 2c), (Supplement Table 3) the mol% $MgCO_3$ ranged from 14.7- 14.9 (Pre 14.8 n=3, Control n=4 14.7, Medium 14.7 n=5, High 14.9 mol% $MgCO_3$ n=5). The new settlement CCA did not have dolomite, i.e. no peak asymmetry, consistent with the absence of white crust underneath.

3.2 Mineral compositional differences between crust layers

As there was no significant difference between treatments, all treatments were combined for each time period. There was a significant difference in Mg composition between experimental crust and pre-experimental crust. Mg-calcite mol% $MgCO_3$ was also significantly different for new settlement (pigmented growth without development of white crust) compared to new crust (growth that has developed white crust). The 6 month new settlement (pigmented growth only) at 14.8 mol% $MgCO_3$ (Fig. 3) was significantly lower than the mol% $MgCO_3$ for the new crusts from the 3 and 6 months new crusts (~16.5 mol% $MgCO_3$). The asymmetry indicating dolomite presence was absent from the new growth, but appeared in new white crust within 3 months (Asymm mol % 17.6) and was higher again for the 6 month new crust (Asymm mol % 18.7). The mol% $MgCO_3$ and asymmetry mol% in the pre-experimental *P. onkodes* crust (the crust formed in the natural environment prior to sample collection) were even higher at 17.5 and 21.6 mol% $MgCO_3$ respectively (Fig. 3) (full data Supplement Table 4).

3.3 SEM results

3.3.1 Comparison of crust across treatments and experimental / pre-experimental

Although there was no detected difference in mineral composition across treatments, SEM was undertaken to visualise potential differences in calcification structures between treatments. There was no visible difference in calcified crust detected between CCA from pre-industrial, control or high CO_2 treatments. There was however, a clear difference

in the structure of the crust grown during the experimental duration compared to the pre-experimental crust (Figs. 4, 5 and supplement Fig. 2). This difference was observed in control CCA, as well as pre-industrial and high CO_2 CCA indicating the difference was not related to the CO_2 levels. Crust formed during the experiment appeared less organized and also appeared structurally less dense (Fig. 6) with cracks and associated gaps in the crust that were not present in the pre-experimental crust. The difference in density was based on observation and not able to be quantified.

The experimental crust had compressed under the action of the saw used to slice the CCA (Fig. 7). We note that this compression by the saw would have made it difficult to identify any differences in growth structure between the CO_2 treatments. Previous work relying on SEM for CCA interpretation has used both saw cutting similarly to here (Nash et al., 2011, 2013a, b; Diaz-Pulido et al., 2014) as well as fracturing without any further treatment of the sample (Nash et al 2013a, Diaz-Pulido et al., 2014). There has not been an observed impact of saw cutting on experimental samples (Diaz-Pulido et al., 2014). However, those previous samples were polished after cutting and fine cracks may have been less obvious due to polishing. The crust features in the pre-experimental crust are comparable to features in other *P. onkodes* analysed using SEM that have been cut, cut and polished or only fractured (Nash et al., 2011, 2013a,b; Diaz-Pulido et al., 2014) and it is unlikely that the use of the saw has introduced an artifact into this study other than to highlight the susceptibility of the experimental crust to crushing compared to pre-experimental crust.

3.3.2 Dolomite features

Dolomite composition determined by SEM-EDS ranged from 37.3 to 59.8 mol% $MgCO_3$ (Table 5 Supplement), comparable to the range identified in previous studies (Nash et al., 2011). There was a de-lineation along the new experimental growth where dolomite was nearly absent compared to consistent infill in pre-experimental crust (Figs 5-7, Supplement Fig. 3). The structure of dolomite formed in the experimental crust also appeared different to that which formed in the pre-experimental crust (Fig. 4). New growth dolomite did not generally fill the cells as was observed in the pre-experimental

growth. In the experimental growth, dolomite was present as lumpy infill or lining (Fig. 4 a and b). In the pre-experimental crust, dolomite lined and in-filled most cells (Fig. 4 c and d). In the control CCA the pre-experimental crust had an opaque organic film that was not visible in experimental growth (Fig. 5c), although there was organic material in the cells (Supplement Fig. 3).

3.3.3 Crust damage possibly due to transfer to experimental tanks

Pre-experimental crust immediately below experimental growth had aragonite cell infill (Fig. 7). In previous work aragonite infill of this type has only been observed at the base of the CCA crust exposed to seawater (Nash et al., 2013a Supplement), or in parts of the skeleton that have been damaged allowing seawater to penetrate. However, we could find no obvious signs of damage to the crust. *P. onkodes* has varied mineralogy throughout the pre-experimental crust (Fig. 8) with patches altered to aragonite and dolomite bands. Regrowth in damaged areas within the pre-experimental crust was more dolomite rich than surrounding areas (Fig. 8b) indicating that damage to crust in the open environment had not resulted in a reduction in dolomite formation.

4 Discussion

Our results show that over the experimental duration 1) there were no changes in any crust mineral composition relating to CO_2 concentrations; 2) CCA bio-mineralised dolomite forms within 12 weeks within aquarium conditions; and 3) CO_2 concentrations do not affect CCA bio-mineralised dolomite formation.

4.1 Magnesium composition and calcification processes

The higher mol% $MgCO_3$ for white crust compared to the pigmented new growth layer (new settlement) has been documented previously for *P. onkodes* (Diaz-Pulido et al.,, 2014). This higher mol% $MgCO_3$ in the white crust suggests that controls on magnesium uptake are different for the white crust (perithallium) than the pigmented surface layers (epithallium).

Considering that CCA crusts are increasingly being used for paleo environmental reconstruction (e.g. Kamenos et al., 2008; Halfar et al., 2013; Caragnano et al., 2014; Darrenougue et al., 2014; Fietzke et al., 2015), it is important to know whether this difference in Mg composition between the pigment surface and white crust is part of the standard calcification processes of the *P. onkodes* or due to post-depositional change. In this and previous work (Nash et al., 2011, 2013a) portions of the crust that have been diagenetically altered post-deposition have cells in-filled by aragonite or Mg-calcite. Typically the cell walls have not exhibited evidence of alteration even when there has clearly been exposure to seawater suggesting the intact cell walls are quite resistant to diagenesis. Probably the epithelial cell walls and perithelial cell walls have differences in the organic material that constrains the Mg uptake. The interfilament and intrafilament (spaces between adjacent cell walls) calcification does not appear to be physically constrained by an organic template in the P. onkodes and *Clathromorphum* Foslie emend (Nash et al., 2013a; Adey et al., 2013). Mg-calcite crystals are randomly orientated or roughly parallel to the cell walls, which suggests that the controls on calcification and consequently Mg incorporation may be different again for the interfilament calcification. It seems most likely that the difference in the mol% $MgCO_3$ for the white crust compared to the pigmented new growth is due to organism-constrained Mg uptake during the crust development. It cannot be determined from this study whether the Mg is incorporated in its final concentrations as the new cell wall and inter/intra filament calcification is first formed or if there is subsequent Mg enrichment over days/weeks/ months. However, previous work subsampling portions of the CCA crust from the top to the base has not demonstrated any systematic increase in mol% $MgCO_3$ (Nash et al., 2013b) suggesting if there is post-deposition Mg enrichment, it occurs relatively contemporaneously with growth.

The consistency of Mg composition across *P. onkodes* and new settlement CCA from pre-industrial to high CO_2 treatments does not provide support for the theory that Mg-C organisms will take up less Mg under higher CO_2 conditions (Andersson et al., 2008). Instead our results agree with the response of *P. onkodes* in an 8 week laboratory

aquarium experiment which also showed no change in mol% $MgCO_3$ in pigmented growth with CO_2 levels up to 1225µatm (Diaz-Pulido et al., 2014). Those CCA were not embedded in resin and were grown in higher temperatures (28 and 30 degrees). Both these aquarium experimental results are in agreement with new settlement CCA in CO_2 enriched flow through systems (Kuffner et al., 2008). This consistency of mol% $MgCO_3$ suggests there is a strong biological control on Mg uptake under variable CO_2 concentrations and no detectable plastic response to CO_2 within the experimental ranges. The absence of change across treatments for mol% $MgCO_3$ in the new settlement CCA, none of which have dolomite, suggests that the similar apparent lack of response of the mol% $MgCO_3$ in the white crusts to CO_2 treatments is unrelated to the presence of dolomite. The lack of difference between pre-industrial, medium and high treatments in the 6 month crust sample set suggests that no trends have been missed with the absence of the control group.

4.2 Comparison to other studies

The results from the *P. onkodes* are in contrast to the decreased Mg composition for tropical branching *Neogoniolithon* sp. (Ries 2011). This form of *Neogoniolithon* is not abundant in the high-energy environments that *P. onkodes* dominates. However, the mol% $MgCO_3$ measured in the *Neogoniolithon* control (~18.7 - 21.3 mol% $MgCO_3$) was much higher and with greater range than that measured for *P. onkodes* in this experiment (pre-experimental crust 17.2-17.9, 3 month crust 16-16.8, new settlement 14.4-15.3 mol% $MgCO_3$ Supplement tables 1, 3 and 4). The mol% $MgCO_3$ in the *Neogoniolithon* decreased to 18.7-16.7 mol% at 903µatm CO_2 (equivalent CO_2 levels as our highest treatment) but only decreased by another 1.3 mol% $MgCO_3$ on average (range 17.3-16.0 mol% $MgCO_3$) with an extra 1962 µatm (2865 µatm CO_2). Thus the lowest Mg levels for the *Neogoniolithon* in the highest CO_2 treatments were comparable to our results for control (and treatments) and to other *P. onkodes* collected from the Great Barrier Reef (Nash et al., 2011; Diaz-Pulido et al., 2014). This raises the possibility that CCA Mg-C levels are susceptible to change as CO_2 rises but only for levels higher than a stable baseline, which for the tropical corallines may be in the range of ~16-17.5 mol% $MgCO_3$. Egilsdottir et al., (2012) working on the temperate articulated coralline

399 *Corallina elongata* reported a significant decrease in Mg content for new structures
400 formed under CO_2 550-1000 µatm. For tips, branches and basal parts formed under the
401 enriched CO_2, Mg content ranged from 14.7 – 15.9 mol% $MgCO_3$ and was not
402 significantly different from controls (15.7, 15.2, 15.4 mol% $MgCO_3$ respectively). On
403 the other hand, structures growing off the base exhibited 16 % $MgCO_3$ under control
404 conditions but reduced in the tips, branches and basal plates of these new structures (15.1,
405 14.9, 15.3 mol% $MgCO_3$) at 550 µatm CO_2. These results suggest there is a different
406 calcification process for the new structures compared to the tips, branches and basal parts
407 and that this calcification process is sensitive to CO_2 but only up to 550 µatm. Research
408 on temperate coralline *Lithothamnion glaciale* showed no change in [Mg] for new growth
409 over 80 days in reduced pH 7.7 treatments (Kamenos et al., 2013).
410
411 Work on CO_2 influences on coralline algae structure has to date been on temperate
412 corallines (e.g. Burdett et al., 2012; Egilsdottir et al., 2012; Ragazzola et al., 2012, 2013;
413 Hofmann et al., 2012; Kamenos et al., 2013). Experiments on living tropical CCA
414 calcification have focused on weight changes (e.g. Anthony et al., 2008; Comeau et al.,
415 2013; Johnson et al., 2014) and impacts on existing crust mineralogy (Diaz-Pulido et al.,
416 2014). There is little specific information known about calcification processes in tropical
417 crustose corallines. However, as this study and previous studies on mineralogy (Nash et
418 al., 2011, 2013b; Diaz-Pulido et al., 2014) show, carbonates in CCA are not only Mg-
419 calcite but can also include dolomite, magnesite and aragonite. It is clear that the net
420 mass of CCA is a result of multiple mineral-forming processes. While all form within the
421 biological structure it seems unlikely that infill dolomite, magnesite and aragonite are all
422 the result of organism controlled calcification processes and instead are biologically
423 induced. Thus experimental net weight changes for *P. onkodes* may not always be a
424 reflection of changes for only Mg-calcite calcification and/or dissolution.
425
426 Aragonite can form as a result of parasitic endolithic bacterial activity within the CCA
427 (Diaz-Pulido et al., 2014) and contribute to measured weight gain. In the Diaz-Pulido et
428 al., study (2014) weight change was due in part to a mix of bacterial-driven carbonate
429 destruction processes and abiotic aragonite precipitation as a result of calcium

mobilisation by the endolithic bacteria. In the Johnson et al., (2014) study weight gain by CCA from locations downstream of the reef front was interpreted as indicating acclimatisation. However, if there were more endolithic bacteria present in their downstream CCA than the reef front CCA, it is possible that the experimental fluctuating conditions with elevated CO_2 activated bacterial processes and the lower CO_2 resulted in increased re-precipitation of mobilised calcium as aragonite (aragonite re-precipitation transforms the porous crust to dense cement) which could account for a proportion of the weight gain. Therefore, it is problematic to presume acclimatisation based on weight gain without knowing how the weight was gained. The published experiments referred to in this discussion were all conducted prior to the discovery of dolomite, magnesite and aragonite in *P. onkodes,* but future studies should consider the more complex nature of mineral composition of *P. onkodes* when attempting to explain weight changes and calcification (e.g. Nash et al., 2013).

The varied responses of the tropical and temperate corallines to altered CO_2 indicate that the uptake of Mg by CCA is not consistent across all species or even within the same organism (Egilsdottir et al., 2012). Furthermore, the use of different methods of measuring Mg concentration potentially complicates comparisons across data sets. Ries (2011) and our study used XRD to determine mol% $MgCO_3$. This measurement only returns mol% for the Mg-Calcite component and is not influenced by the presence of Mg in other forms, e.g. dolomite or within organics, or diluted by the presence of aragonite. Kamenos et al., (2013) used Raman spectroscopy for identifying mol% $MgCO_3$ changes, this method is not widely used for coralline algae mineralogy studies. Egilsdottir et al., (2012) used inductively coupled plasma- atomic emission spectroscopy (ICP-AES) to quantify bulk Mg and Ragazzola et al., (2013) used electron microprobe to obtain an average elemental composition for Mg/Ca ratios. These methods return bulk Mg for the total sample or portion under the electron beam and may be skewed by undetected aragonite, common in corallines (Smith et al., 2012; Nash et al., 2013b) or presence of Mg not within the Mg-calcite, (e.g. Caragnano et al., 2014).

4.3 Dolomite formation within 12 weeks

461 Prior to the discovery of bio-mediated dolomite in association with bacteria (Vasconcelos
462 and Mackenzie 1997) and CCA (Nash et al., 2011,) dolomite was thought to form by
463 chemical alteration of limestone over geological time frames, e.g. thousands to millions
464 of years (e.g. Saller 1984). Although it has also been controversially argued that
465 dolomite was the primary precipitation in some ancient dolomite formations (Tucker
466 1982). Our experimental results demonstrate that bio-mineralised dolomite formation is
467 rapid and occurring contemporaneously with the surrounding limestone formation. The
468 apparent reduction in dolomite formation in the experimental conditions compared to the
469 pre-experimental growth indicates that there is also a rapid response to changing
470 environmental conditions. Accordingly, any interpretation of past environments made
471 using dolomite that may have had a biological origin, i.e. dolomite in formerly shallow
472 tropical environments, would need to take into account this potentially rapid formation
473 and response to environmental change.
474
475 **4.4 Implications for interpreting the geological past**
476 The absence of a significant effect of CO_2 on dolomite formation in this experiment
477 suggests that the observed correlation in the geologic rock record of dolomite and
478 greenhouse conditions may not be a direct result of high CO_2 driving increased primary
479 bio-mineralised dolomite formation. However, as noted in previous work (Nash et al.,
480 2013a; Diaz-Pulido et al., 2014) dolomite is more resistant to chemical dissolution and
481 biological erosion than Mg-calcite (and presumably also calcite). Therefore, the positive
482 correlation of dolomite and greenhouse epochs in the rock record (e.g. MacKenzie et al.,
483 2008; Wilkinson and Given 1986) may be due in part to preferential preservation of bio-
484 mineralised dolomite compared to surrounding skeletal material, rather than CO_2 or
485 temperature driven biological processes leading to increased dolomite formation.
486 Furthermore, during greenhouse times, sea level was higher thereby providing greater
487 area of warm shallow (epeiric) seas and thus more accommodation space for calcifying
488 algae that may have formed dolomite. While past primary bio-mineralised dolomite
489 levels may not have been directly linked to CO_2 levels, there is certainly support from
490 other work (Nash et al., 2013a; Diaz-Pulido et al., 2014) for indirect biologically-

associated processes leading to increased abundance of bio-mineralised dolomite under higher CO_2 conditions.

4.5 Changes in calcification in experimental tanks

Considering the aragonite observed in the crust where the CCA was transferred to the experimental tanks, it may be that interruptions to normal growth after transfer to experimental tanks, allowed seawater to penetrate into the shallow surface layer resulting in alteration of Mg-C to aragonite. Previous experiments on calcification rates of CCA found that rates of photosynthesis, and production of inorganic and organic carbon, were significantly lower in experimental tanks than *in situ* (Chisholm, 2003). A decrease in photosynthesis and calcification rates may be the explanation for the observed differences in calcified crust in this study, although the exact mechanism leading to the change is not known. The absence of the organic film in the experimental growth (Fig. 5c) raises the possibility that it is the absence of these organics that has led to the observed differences in calcification. This organic film is consistently present on the pre-experimental growth and consistently absent from the experimental growth. Thus it is unlikely to be a sample preparation artifact, although the preparation method may make this film more readily visible than if the samples had been fractured leaving an uneven surface. Reduced organic production may also lead to less dolomite as experiments have shown that dolomite nucleates on polysaccharides produced by red algae (Zhang et al., 2012). It is probable that our experimental results understate how much dolomite could be formed in the open marine environment over a 3 and 6 month period.

The observation that the change to experimental tanks coincided with changes in CCA calcification has implications for extrapolating experimental results back to the natural environment. There is a substantial change in the ultrastructure and secondary mineralisation (i.e. formation of dolomite) processes. While comparisons between treatments are reliable, exact rates of calcification for *P. onkodes* are likely to be understated in experimental conditions compared to the open reef. This is an area that requires further work to determine what is causing this difference in calcification and if it is common to all similar experiments. Flow and wave energy will be important factors

522 that influence the calcification processes and should also be considered in future
523 aquarium designs that seek to test the effects of future acidification scenarios on CCA's.
524
525 **4.6 What does Mol% Mg-calcite mean for the CCA physiology and reef**
526 **processes in a changing climate?**
527 There have been no studies to date that explore the drivers of organism-controlled
528 calcification in the key reef-builder *P. onkodes* and what role the Mg content plays in
529 this. Thus it is unclear at this time what influence the mol% $MgCO_3$ has on CCA
530 physiology and reef processes and even more difficult to anticipate what may happen in
531 the future in a changing climate. Early studies on Mg-C CCA dissolution rates (Plummer
532 and Mackenzie 1974; Bischoff et al., 1987) used CCA that had dolomite and possibly
533 magnesite (see Nash et al., 2013 for discussion). Those results were a mix of dissolution
534 rates for the 2-3 different Mg minerals, not just for Mg-calcite with different phases of
535 mol% $MgCO_3$ as was interpreted. Much of our present understanding of biogenic Mg-C
536 dissolution is based on those interpretations (e.g. Andersson et al., 2008). Considering
537 how recent work on CCA dissolution has revealed that a complex suite of interacting
538 mineral, biological, bacterial and chemical factors contribute to net dissolution responses
539 (Nash et al., 2013; Reyes-Nivia et al., 2014; Diaz-Pulido et al., 2014) it has become
540 apparent that the prevailing theory that higher Mg content leads to lower stability is
541 probably not applicable to tropical *P. onkodes*. Indeed there have been no dissolution
542 experiments comparing the dissolution rates of CCA with different mol% $MgCO_3$ to test
543 the correlation of dissolution rates to Mg content of Mg-C.

544

545 **4.7 Implications for reef management**
546 Finding that dolomite is not affected by ocean acidification in these 3 and 6 month
547 experiments is good news for the survival of CCA species *P. onkodes* under predicted
548 ocean acidification conditions. Dolomite confers stability on the CCA and facilitates its
549 reef-building role (Nash et al., 2013a) as well as being resistant to bacterial bio-erosion
550 (Diaz-Pulido et al., 2014). At this time exact drivers of CCA dolomite formation have not
551 been identified. It seems most likely that dolomite formation is related to provision of a
552 suitable organic substrate, probably being the polysaccharides derived from red algae for

agar (Nash et al., 2013a; Zhang et al., 2012). For coral reef management, it is necessary to understand what environmental conditions negatively impact dolomite formation. CCA crust formation is likely to suffer negative affects from reduced recruitment, increased bleaching, bio-erosion and dissolution under higher CO_2 and temperatures (Kuffner et al., 2011; Diaz-Pulido et al., 2012). However, understanding the conditions that negatively impact dolomite formation may enable more effective assessments of the risk that CO_2-driven ocean acidification may pose to important reef-builders such as *P. onkodes*. Identifying the drivers and constraints of CCA dolomite formation is an area of research that has not yet been initiated and as such, there is a long way to go to understand what conditions may negatively impact on CCA dolomite formation.

Acknowledgements

Thanks to Frank Brink and the Centre for Advanced Microscopy at the Australian National University for assistance with SEM. Thanks to Florita Flores, Michelle Liddy, Julia Strahl, Paulina Kaniewska and Jordan Hollarsmith for aquarium maintenance and experimental assistance. Funding for the experimental work was provided by the Australian Institute of Marine Science and a Super Science Fellowship from the Australian Research Council. Support for mineral analysis was provided by the Electronic Materials Engineering department at the Research School of Physics, Australian National University.

References

Adey, W. H., Halfar, J., and Williams, B.: The coralline genus Clathromorphum Foslie emend. Adey: Biological, physiological, and ecological factors controlling carbonate production in an Arctic-Subarctic climate archive. Smithsonian contributions to the marine sciences; number 40, 2013.

584 Andersson, A. J., Mackenzie, F. T., Bates, N. R.: Life on the margin: implications of
585 ocean acidification on Mg-calcite, high latitude and cold-water marine calcifiers,
586 Mar. Ecol. Prog. Ser, 373, 265-273, 2008.
587
588 Anthony, K. R. N., Kline, D. I., Diaz-Pulido, G., Dove, S., Hoegh-Guldberg, O.: Ocean
589 acidification causes bleaching and productivity loss in coral reef builders, PNAS
590 105, 17442-17446, 2008.
591
592 Bischoff, W. D., Mackenzie, F. T., Bishop, F. C.: Stabilities of synthetic magnesian
593 calcites in aqueous solution: Comparison with biogenic materials, Geochim.
594 Cosmochim. Acta. 51, 1413–1423, 1987.
595
596 Burdett, H. L., Hennige, S. J., Francis, F. T. Y., and Kamenos, N. A.: The photosynthetic
597 characteristics of red coralline algae, determined using pulse amplitude
598 modulation (PAM) fluorometry, Mar. Biol. Res., 8, 756-763, 2012.
599
600 Caragnano, A. D., Basso, D. E., Jacob, D., Storz, G., Rodondi, F., Benzoni, Dutrieux, E.:
601 The coralline red alga *Lithophyllum kotschyanum* f. *affine* as proxy of climate
602 variability in the Yemen coast, Gulf of Aden (NW Indian Ocean), Geochim
603 Cosmochim Ac
604 124,1-17, 2014.
605
606 Chisholm, J. R. M., Primary productivity of reef-building crustose coralline algae,
607 Limnol. Oceanogr, 48,1376-1387, 2003.
608
609 Comeau, S., Edmunds, P. J., Spindel, N. B., Carpenter, R. C.: The responses of eight
610 coral reef calcifiers to increasing partial pressure of CO2 do not exhibit a tipping
611 point, Limnol. Oceanogr, 58, 388-398, 2013.
612

613 Darrenougue, N., De Deckker, P., Eggins, S., & Payri, C: Sea-surface temperature
614 reconstruction from trace elements variations of tropical coralline red algae.
615 Quaternary Science Reviews, 93, 34-46, 2014.
616
617 Diaz-Pulido, G., Anthony, K., Kline, D. I., Dove, S., Hoegh-Guldberg, O.: Interactions
618 between ocean acidification and warming on the mortality and dissolution of
619 coralline algae, J. Phyc, 48, 32-39, 2012.
620
621 Diaz-Pulido, G., Nash, M. C., Anthony, K. R. N., Bender, D., Opdyke, B. N., Reyes-
622 Nivia, C., Troitzsch, U.: Greenhouse conditions induce mineralogical changes and
623 dolomite accumulation in coralline algae on tropical reefs, Nat Comms, 5,2014.
624
625 Egilsdottir, H., Noisette, F., Noel, L. M., Olafsson, J., Martin, S.: Effects of pCO2 on
626 physiology and skeletal mineralogy in a tidal pool coralline alga *Corallina*
627 *elongate,* Mar Biol, 160, 2103-2112, 2012.
628
629 Fietzke, J., Ragazzola, F., Halfar, J., Dietze, H., Foster, L. C., Hansteen, T. H.,
630 Eisenhauer, A., and Steneck., R. S.: Century-scale trends and seasonality in pH
631 and temperature for shallow zones of the Bering Sea. P. Natl. Acad. Sci., 112,
632 2960-2965, 2015
633
634 Gaines, A.: Protodolomite redefined, J. Sed. Pet, 47, 543-546, 1977
635
636 Given, R. K., Wilkinson, B. H.: Dolomite abundance and stratigraphic age: constraints on
637 rates and mechanisms of Phanerozoic dolostone formation, J Sediment Petrol 57,
638 1068-1078, 1987.
639
640 Halfar, J., Adey, W. H., Kronz, A., Hetzinger, S., Edinger, E., and Fitzhugh, W. W.:
641 Arctic sea-ice decline archived by multicentury annual-resolution record from
642 crustose coralline algal proxy. P. Natl. Acad. Sci., 110, 19737-19741, 2013.
643

644 Hofmann, L. C., Yildiz, G., Hanelt, D., Bischof, K.: Physiological responses of the
645 calcifying rhodophyte, *Corallina officinalis* (L.), to future CO2 levels, Mar Biol,
646 159, 783-792, 2012.
647
648 Howard, W. R., Nash, M., Anthony, K., Schmutter, K., Bostock, H., Bromhead, D., …
649 Williamson, J.: Ocean acidification. *In* A Marine Climate Change Impacts and
650 Adaptation Report Card for Australia 2012, *Edited by* Poloczanska E, Hobday A,
651 Richardson A. Centre for Australian Weather and Climate Research, Hobart,
652 TAS,2012.
653
654 Jones, B., Luth, R. W., McNeil, A. J.: Powder X-ray diffraction analysis of homogeneous
655 and heterogeneous sedimentary dolostones, J. Sed. Res. 71, 790-799, 2001.
656
657 Johnson, M. D., Moriarty, V. W., Carpenter, R. C.: Acclimatization of the Crustose
658 Coralline Alga Porolithon onkodes to variable pCO2, PLoS ONE 9, e87678,
659 2014.
660
661 Kaczmarek, S. E., and Sibley, D. F.: On the evolution of dolomite stoichiometry and
662 cation order during high-temperature synthesis experiments: An alternative model
663 for the geochemical evolution of natural dolomites, Sed. Geol. 240, 30-40, 2011.
664
665 Kamenos, N. A., Cusack, M., and Moore, P. G.: Coralline algae are global
666 palaeothermometers with bi-weekly resolution. Geochim. Cosmochim.
667 Acta, 72(3), 771-779, 2008.
668
669 Kamenos, N. A., Burdett, H. L., Aloisio, E., Findlay, H. S., Martin, S., Longbone, C.,
670 Dunn, J., Widdicombe, S., and Calosi, P.: Coralline algal structure is more
671 sensitive to rate, rather than the magnitude, of ocean acidification, Global Change
672 Biology, 19, 3621-3628, 2013.
673

674 Kuffner, I. B., Andersson, A. J., Jokiel, P. L., Rodgers, K. S., Mackenzie, F. T.:
675 Decreased abundance of crustose coralline algae due to ocean acidification, Nat
676 Geoscience, 1, 114-117, 2007.
677
678 Morse, J. W., Arvidson, R. S., Lüttge, A.: Calcium carbonate formation and dissolution,
679 Chem Rev, 107, 342-381, 2007.
680
681 Nash, M. C., Troitzsch, U., Opdyke, B. N., Trafford, J. M., Russell, B. D., Kline, D.
682 I.:First discovery of dolomite and magnesite in living coralline algae and its
683 geobiological implications, Biogeosciences, 8, 3331-3340, 2011.
684
685 Nash, M. C., Opdyke, B. N., Troitzsch, U., Russell, B. D., Adey, W. H., Kato, A., ...
686 Kline, D. I., Dolomite-rich coralline algae in reefs resist dissolution in acidified
687 conditions, Nat Climate Change, 3, 268-272, 2013a.
688
689 Nash, M. C., Opdyke, B. N., Wu, Z., Xu, H., Trafford, J. M.: Simple x-ray diffraction
690 techniques to identify mg-calcite, dolomite, and magnesite in tropical coralline
691 algae and assess peak asymmetry, J Sediment Res 83, 1085-1099, 2013b.
692
693 Pueschel, C. M., Judson, B. L., and Wegeberg, S. : Decalcification during epithallial cell
694 turnover in Jania adhaerens (Corallinales, Rhodophyta).Phycologia, 44,156-162,
695 2005.
696
697 Ramirez-Reinat, E. L., and Garcia-Pichel, F.: Characterization of a marine
698 cyanobacterium that bores into carbonates and the redescription of the genus
699 Mastigocoleus, J. Phycol. 48, 740-749, 2012.
700
701 Ries, J. B.: Skeletal mineralogy in a high CO2 world, J. Exp. Mar. Biol. Ecol. 403, 54-64,
702 2011.
703

Mackenzie, F. T., Arvidson, R. S., Guidry, M. W.: Chemostatic models of the ocean atmosphere-sediment system through Phanerozoic time, Mineral Mag. 72, 329-332, 2008.

Orr, J.: Recent and future changes in ocean carbonate chemistry, in Ocean Acidification (eds Gattuso JP, Hansson L) Chpt 3, 41-66, 2011.

Plummer, L. N., Mackenzie, F. T.: Predicting mineral solubility from rate data: Application to the dissolution of magnesian calcites, Am. J. Sci. 274, 61–83, 1974.

Ragazzola, F., Foster, L. C., Form, A., Anderson, P. S., Hansteen, T. H., Fietzke, J.: Ocean acidification weakens the structural integrity of coralline algae, Glob Change Biol, 18, 2804-2812, 2012.

Ragazzola, F., Foster, L. C., Form, A. U., Buscher, J., Hansteen, T. H., Fietzke, J.: Phenotypic plasticity of coralline algae in a high CO_2 world, Ecol Evol 3, 3436-3446, 2013.

Reyes-Nivia, C., Diaz-Pulido, G., Dove, S.: Relative roles of endolithic algae and carbonate chemistry variability in the skeletal dissolution of crustose coralline algae, Biogeosciences Discussions 11, 2993-3021, 2014.

Saller, A. H.: Petrologic and geochemical constraints on the origin of subsurface dolomite, Enewetak Atoll: An example of dolomitization by normal seawater, Geology, 12, 217-220. 1984.

Smith, A. M., Sutherland, J. E., Kregting, L., Farr, T. J., Winter, D. J.: Phylomineralogy of the Coralline red algae: Correlation of skeletal mineralogy with molecular phylogeny, Phytochemistry, 81, 97-108, 2012.

735 Steneck, R. S.: The ecology of coralline algal crusts: convergent patterns and adaptative
736 strategies. Annual Review of Ecology and Systematics, 273-303, 1986.
737
738 Tucker, M. E.: Precambrian dolomites: petrographic and isotopic evidence that they
739 differ from Phanerozoic dolomites, Geology, 10, 7-12, 1982.
740
741 Uthicke, S., Pecorino, D., Albright, R., Negri, A. P., Cantin, N., Liddy, M., Dworjanyn,
742 S., Kamya, P., Byrne, M., Lamare, M.: Impacts of Ocean Acidification on Early
743 Life-History Stages and Settlement of the Coral-Eating Sea Star *Acanthaster*
744 *planci*, PLoS ONE 8, e82938, 2013.
745
746 Vasconcelos, C., McKenzie, J. A.: Microbial mediation of modern dolomite precipitation
747 and diagenesis under anoxic conditions (Lagoa Vermelha, Rio de Janeiro, Brazil),
748 J Sediment Res, 67, 378-390, 1997.
749
750 Wilkinson, B. H., Given, R. K.: Secular variation in abiotic marine carbonates:
751 Constraints on Phanerozoic atmospheric carbon dioxide contents and oceanic
752 Mg/Ca ratios, J. Geol, 94, 321-333, 1986.
753
754 Zhang, F., Xu, H., Konishi, H., Shelobolina, E. S., Roden, E. E.: Polysaccharide-
755 catalyzed nucleation and growth of disordered dolomite: A potential precursor of
756 sedimentary dolomite, Am Mineral, 97, 556-567, 2012.
757
758 Zhang, F., Xu, H., Shelobolina, E. S., Konishi, H., Converse, B., Shen, Z., and Roden, E.
759 E.: The catalytic effect of bound extracellular polymeric substances excreted by
760 anaerobic microorganisms on Ca-Mg carbonate precipitation: Implications for the
761 “dolomite problem”. Am. Mineral.,100, 483-494, 2015.
762
763 Zhao, H., and Jones, B.: Origin of “Island dolostones”: a case study from the Cayman
764 Formation (Miocene), Cayman Brac, British West Indies, Sed. Geol. 243-244,
765 191-206, 2012.

766
767
768 **Figure Legends**
769 **Table 1:** Two factor analysis of variance (ANOVA) testing for difference in mol%
770 $MgCO_3$ and Asymmetry indicating dolomite, between different CO_2 treatments (Factor
771 Treatment) and experimental growth versus pre-experimental growth (Factor Type). No
772 significant difference related to CO_2 treatments, but significant difference between
773 experimental and pre-experimental growth for both mol% $MgCO_3$ and dolomite
774 asymmetry.

775 **Figure 1:** Example of *P. onkodes* after 3 months. New pigmented crust overgrowing
776 resin used for XRD.

777 **Figure 2:** Magnesium composition for experimental growth of *P. onkodes*. Mol% is for
778 Mg-calcite mol% $MgCO_3$. Asymm mol% includes influence of dolomite asymmetry on
779 calculated Mg-calcite mol% $MgCO_3$, the more dolomite present the higher the Asymm
780 mol%. **(a)** New crust after 3 months. **(b)** New crust after 6 months. There was no
781 significant difference between treatments for either the mol% $MgCO_3$ or the Asymm
782 mol% in new crust after 3 or 6 months. 782Δ control samples were unavailable for
783 mineral analyses. **(c)** New settlement after 6 months. As for the new crust, there was no
784 significant difference across the treatments in mol % $MgCO_3$. There is no dolomite in the
785 new settlement consistent with the absence of white crust. Error bars are ± 1 s.d.

786 **Figure 3:** Magnesium composition for CCA new settlement, 3 month crust, 6 month
787 crust, and pre-experimental crust. The mol% $MgCO_3$ in the Mg-calcite increases from
788 new settlement to 3 and 6 months, and again for the pre-experimental crust. Dolomite is
789 not present in the new settlement, appears within 3 months, increases in amount in the 6
790 month new crust, but is highest in the pre-experimental crust. Error bars are 1 s.d.

791 **Figure 4:** SEM (Backscatter -BSE) of control *P. onkodes* showing dolomite in
792 experimental and pre-experimental growth. BSE SEM shows the lighter elements i.e.
793 magnesium, as darker gray and heavier elements, i.e. calcium is pale gray to white.
794 Secondary electron images show the topography of the sample but do not provide

information on the elemental composition. EDS measurements are made in the different gray shade areas to measure Mg composition (range listed in supplement) and this is used to identify the mineral composition. Once the measurements have been made it is possible then to identify dolomite and calcite from the gray shade. **(a)** Experimental growth- dolomite (D) Dolomite-composition material in cell. This is not the typical cell lining but has been observed in other CCA. Mg-calcite (Mg-C). Scale = 2 microns. **(b)** Experimental growth: micro-scale lumpy dolomite lining cell. Scale = 1 micron. Cell growth in experimental growth is less regular and organized than pre-experimental growth. **(c)** Dolomite cell lining in pre-experimental growth. Notice the very narrow cell walls. **(d)** Dolomite infill in a reproductive conceptacle in the old growth. Cells below conceptacle are all in-filled with dolomite. Scale bars: a and c = 2 microns, b = 1 micron, d = 10 microns.

Figure 5: Control *P. onkodes* with experimental growth on pre-experimental growth. **(a)** (BSE) There is a visible difference in the appearance of experimental crust (black arrow) to the pre-experimental growth (black dashed arrow). The lighter grey of the surface is due to less magnesium (dolomite) infilling the cells that appear as darker grey infill in the pre-experimental lower part of the crust. Black box enlarged in **b**. D is dolomitised conceptacle. **(b)** Close up showing the consistent presence of infill in pre-experimental growth whereas in the new growth regular dolomite cell lining is absent. Also, the Mg-C crust itself appears to be less dense with many cracks from the cutting visible in the new growth but not so in the pre-experimental growth. **(c)** Secondary electron image of control CCA. The pre-experimental growth appears to have a fine opaque organic film covering part of the cut crust (white dashed arrow), but this is not present in the experimental growth (White arrow). **(d)** Control CCA (BSE) Dashed arrow to pre-experimental growth. Grey cells are dolomite infill. Black arrow to experimental growth, generally an absence of dolomite infill, note line of porosity in transition between pre-experimental and experimental growth. Scale bars: a, c and d = 100 microns, b = 20 microns.

Figure 6: Transition from pre-experimental crust to experimental crust in *P. onkodes*, pre-industral CCA **(a, b) (BSE)**, high CO_2 CCA **(c, d)**. Transition from pre-experimental

growth to experimental identified by following the growth lines from the crust on the resin (not pictured) across the sample. **(a)** overview, brackets- new growth. **(b)** close up of transition. Crust below dashed line is pre-experimental growth. Dolomite infills cells (black arrows). Above dashed line new growth does not have cells infilled, crust has been damaged by saw cut. **(c)** Overview of transition to new growth in high CO_2 CCA, brackets – new growth. **(d)** close up of transition. Similarly to control and pre-industrial CCA, cells in pre-experimental growth are infilled with dolomite (black arrows). Crust above dashed line grew during experiment. Cells are not infilled with dolomite and crust has crushed under the sawcut. Scale bars a, b, c and d = 20 microns. Close up of transition between from pre-experimental growth to experimental growth in supplement Fig. 3.

Figure 7: SEM (BSE) of Control *P. onkodes* (AC4). **(a)** Overview of experimental growth, pre-experimental growth and transition zone (bracket). Cells at the surface do not have dolomite. White box enlarged in B. **(b)** Cells in experimental growth have no dolomite infill. Cells below experimental growth have dolomite lining the cells but the centres are in-filled with aragonite. White box enlarged in C, black box enlarged in E. **(c)** close up of cell infill by aragonite within the dolomite lining. **(d)** Dolomite lined cell in transition zone with aragonite infill. **(e)** Patch of crust below experimental growth with aragonite infill. **(f)** Close up of dolomite-lined cell with aragonite infill. Scale bars: a and b = 20 microns, c and f = 1 micron, d = 2 microns, e = 10 microns.

Figure 8: SEM (BSE) of varied mineral fabrics in CCA. **(a)** Alteration of base of CCA crust by bacteria to aragonite (Diaz-Pulido et al., 2014), remnant CCA cells are visible in the aragonite (A) confirming it was CCA crust and not coral substrate. **(b)** Hypothallus cells grow parallel to substrate then grow vertically and are in-filled with dolomite (D). In-fill of micro-borer trace by aragonite and dolomite rim (arrow). **(c)** Band of dolomite between aragonite alteration and undamaged cells. (**d**) Damaged crust has been in-filled with new cell growth rich in dolomite. Scale bars: a = 100 microns, b, c and d = 20 microns.

	Mol %				Asymmetry			
	DF	MS	F	p	DF	MS	F	p
Treatment	2	1.76E-05	0.77	0.4754	2	1.98E-04	0.55	0.582
Type	1	6.52E-04	28.54	**< 0.001**	1	7.00E-03	19.57	**<0.001**
Tr X Type	2	0.49	0.61972	0.1195	2	0.35	0.7082	0.099
Residual	21				22	3.58E-04		

855

856 Table 1

857

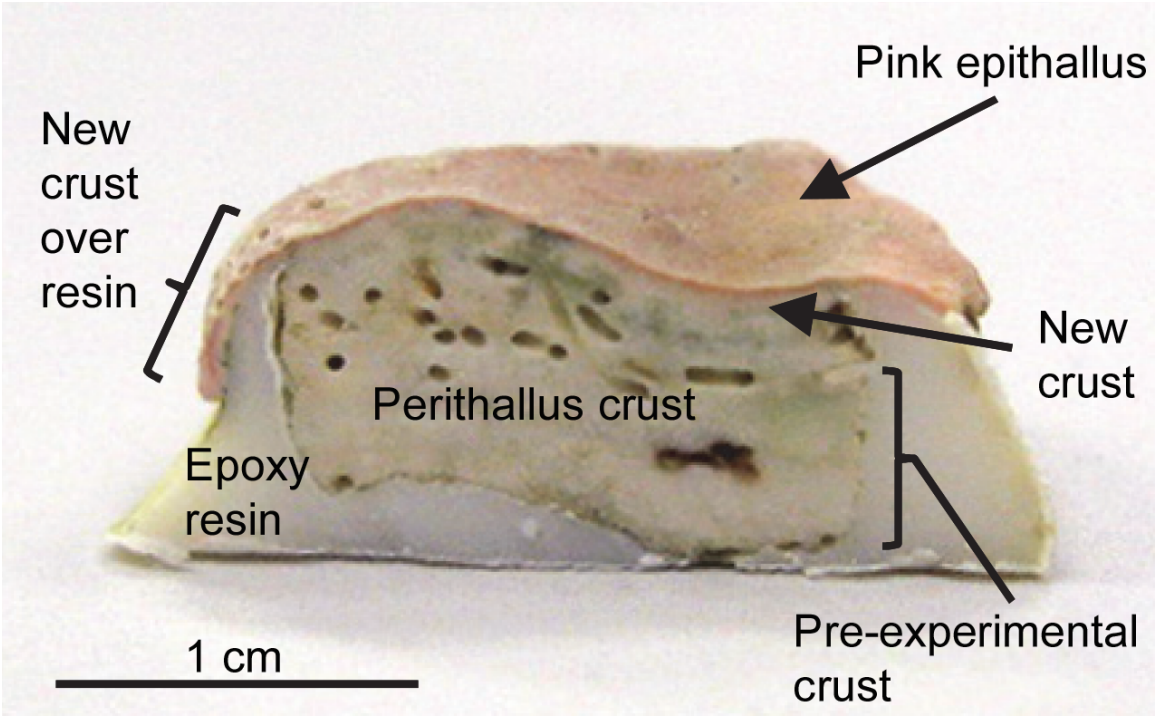

858

859 Figure 1

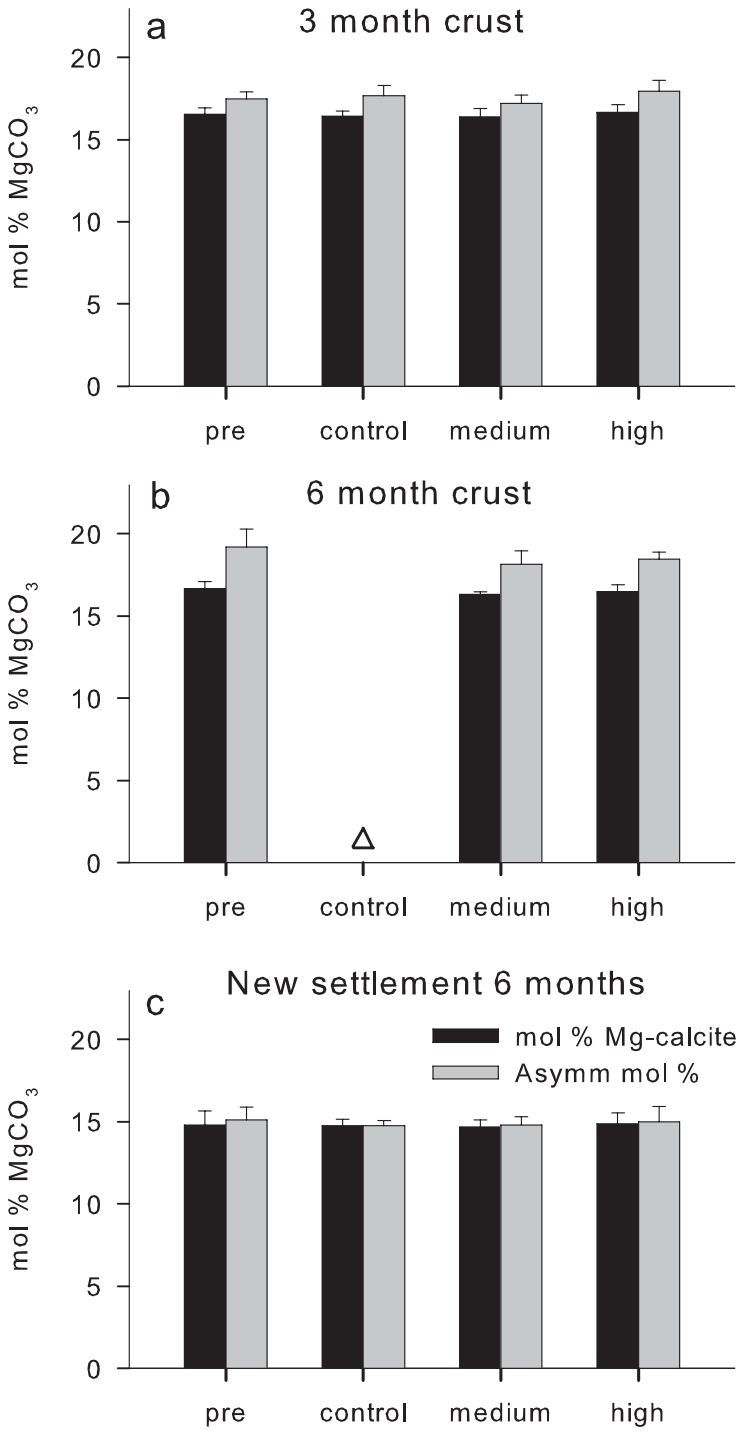

860

861 **Figure 2**

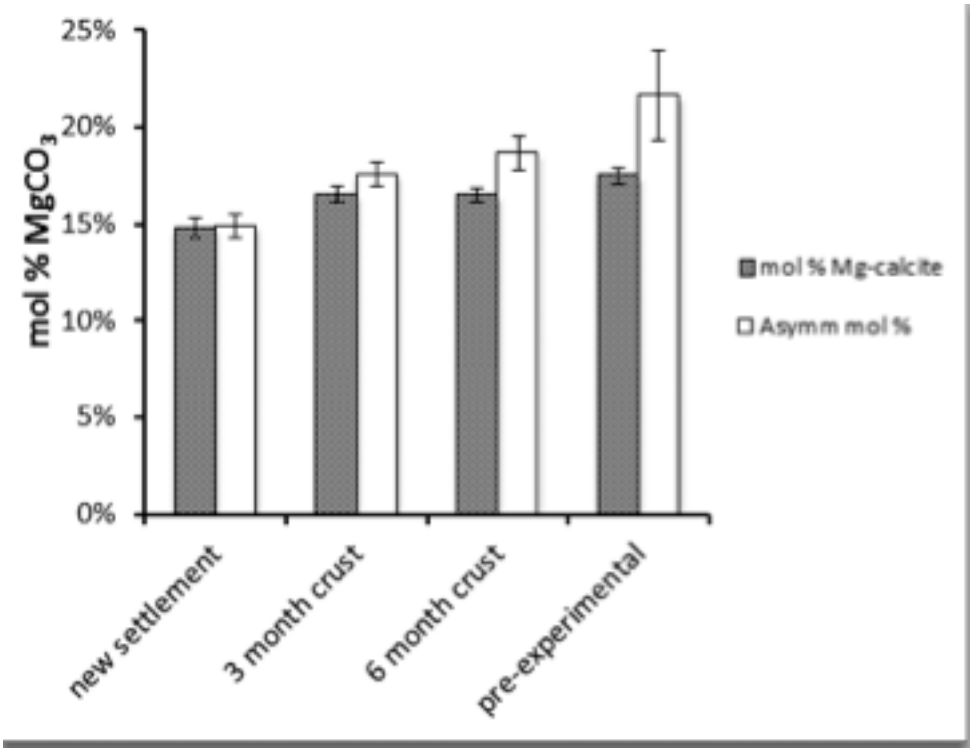

862

863 **Figure 3**

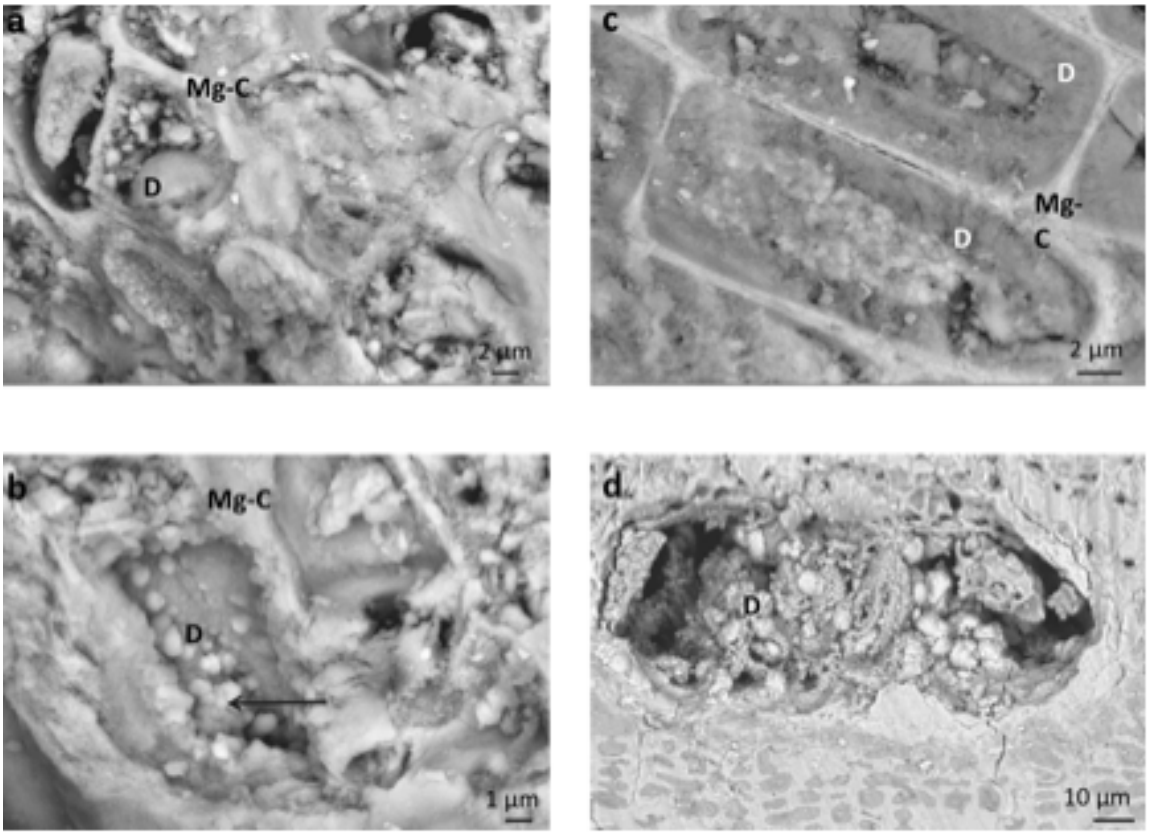

864

865 **Figure 4**

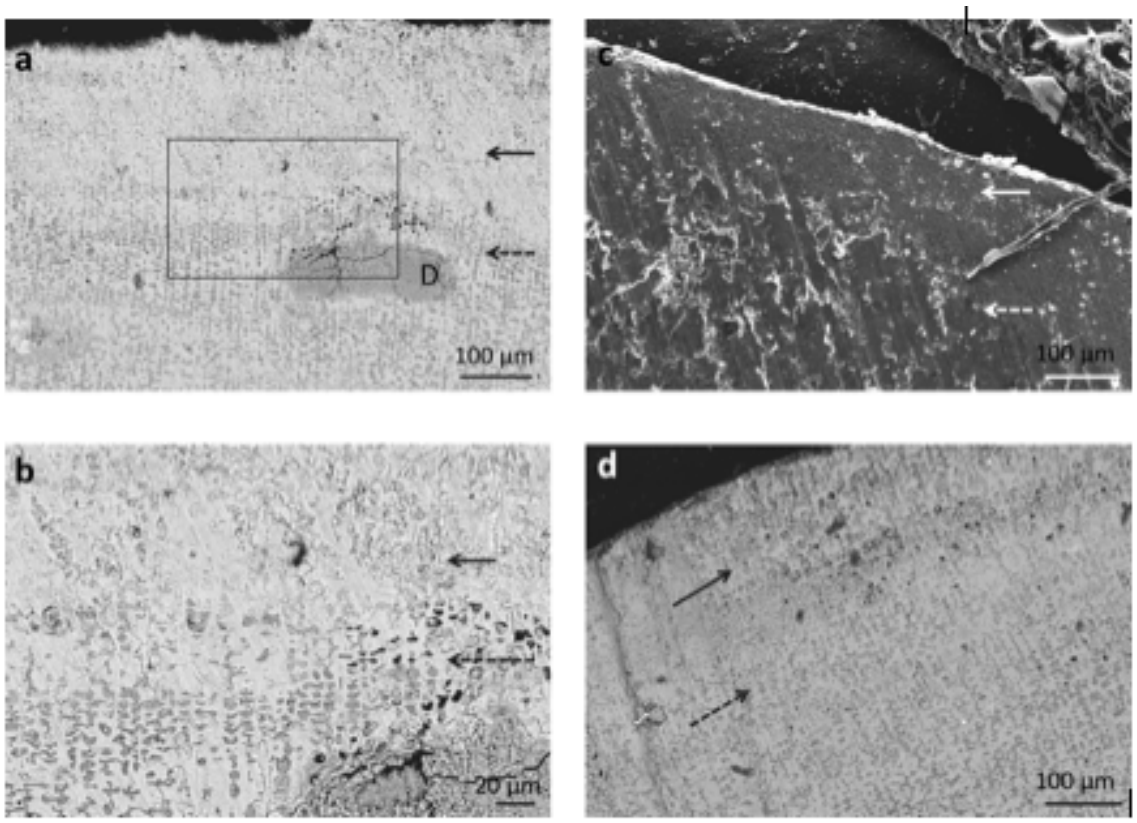

Figure 5

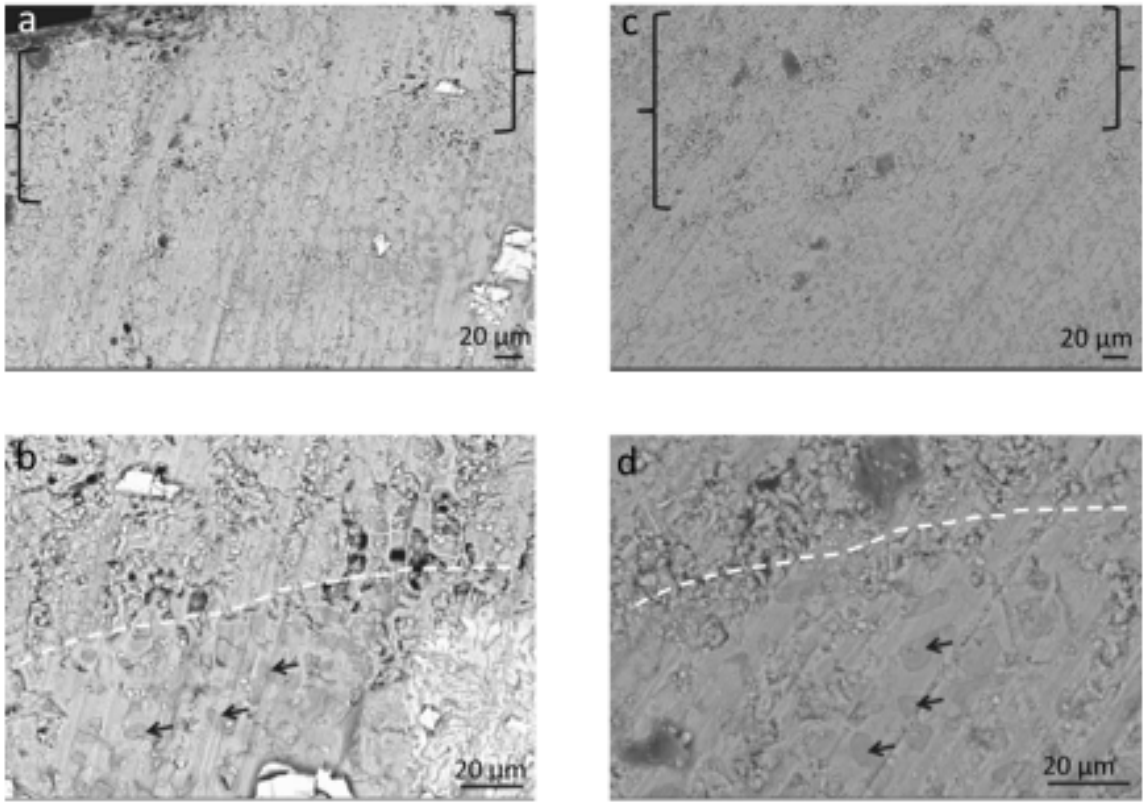

869 **Figure 6**

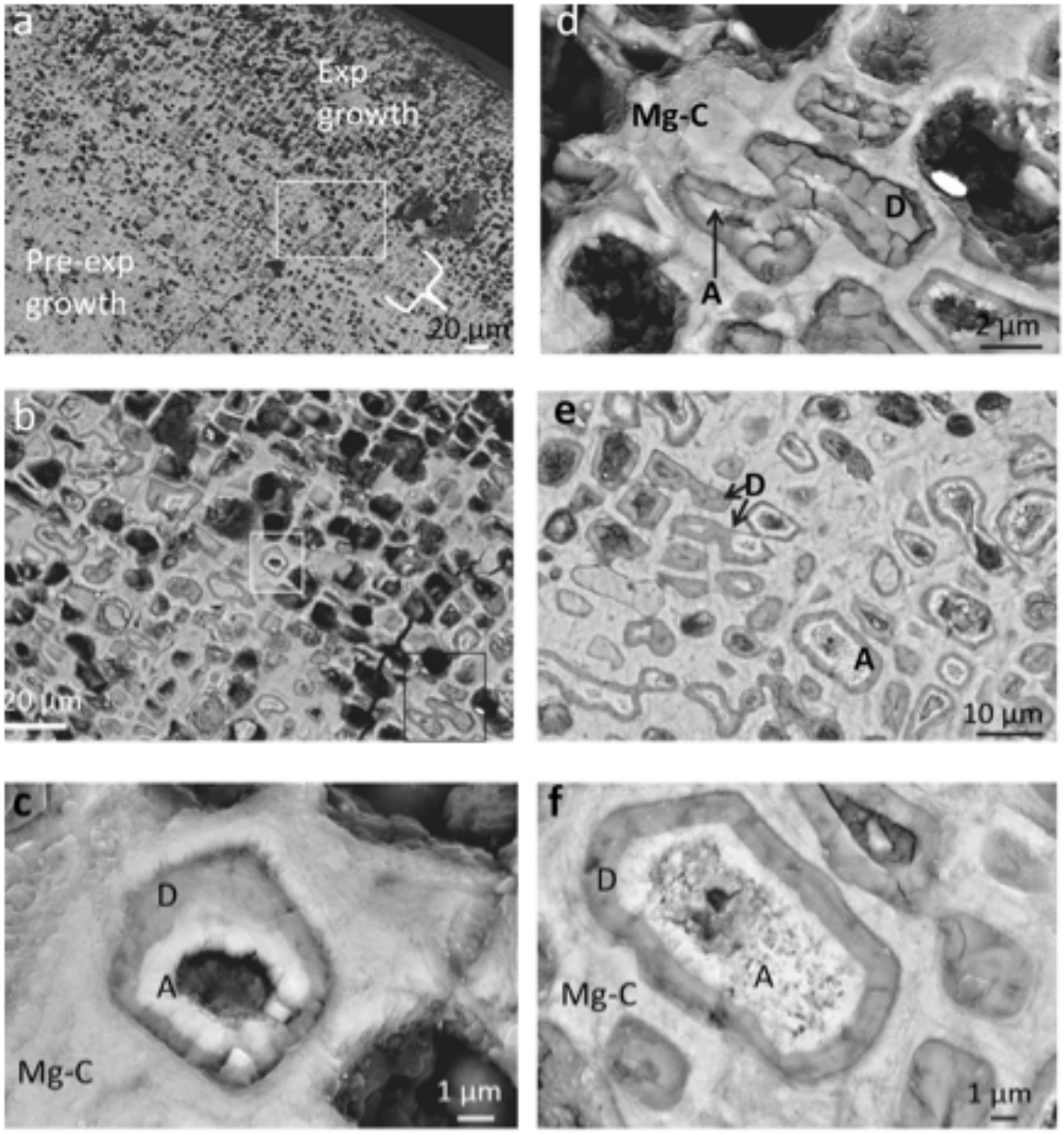

870

871 **Figure 7**

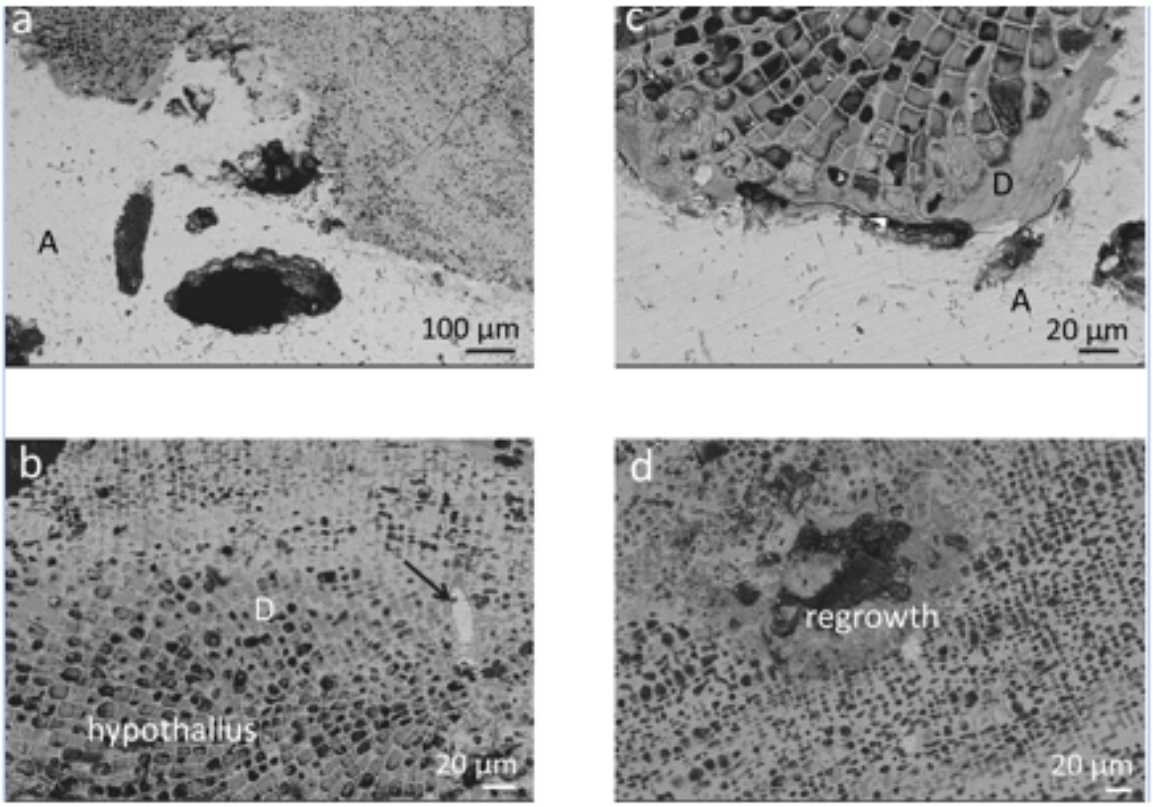

Figure 8